Chemosphere 197 (2018) 262–270

Contents lists available at ScienceDirect

Chemosphere

journal homepage: www.elsevier.com/locate/chemosphere

Mercury in a stream-lake network of Andean Patagonia (Southern Volcanic Zone): Partitioning and interaction with dissolved organic matter

Carolina Soto Cárdenas [a, *], María del Carmen Diéguez [a], Claudia Queimaliños [a], Andrea Rizzo [b, c], Vesna Fajon [d], Jože Kotnik [d], Milena Horvat [d], Sergio Ribeiro Guevara [b]

[a] Grupo de Ecología de Sistemas Acuáticos a escala de Paisaje, Instituto de Investigaciones en Biodiversidad y Medioambiente (INIBIOMA, UNComahue- CCT Patagonia Norte CONICET), Quintral 1250, 8400, San Carlos de Bariloche, Río Negro, Argentina
[b] Laboratorio de Análisis por Activación Neutrónica, Comisión Nacional de Energía Atómica, Centro Atómico Bariloche, Av. Bustillo km 9.5, 8400 Bariloche, Argentina
[c] CCT Patagonia Norte CONICET Av. Pioneros 2350, 8400, Bariloche, Argentina
[d] Department of Environmental Sciences, Jožef Stefan Institute, Jamova 39, SI-1000 Ljubljana, Slovenia

HIGHLIGHTS

- High THg levels were found in a stream-lake network placed within a volcanic area.
- High THg:DOC ratios determined high Hg^{2+} binding to abiotic and biotic particles.
- Stream Hg species are related to terrestrial DOM, reflecting inputs from the catchment.
- Lake Hg speciation related to DOM quality and photochemical and biological processes.
- Hg^0 was higher in the upper lake layers due to photo- and biological reduction.

GRAPHICAL ABSTRACT

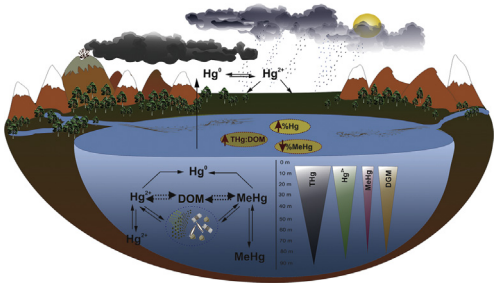

ARTICLE INFO

Article history:
Received 10 November 2017
Received in revised form
10 January 2018
Accepted 11 January 2018
Available online 12 January 2018

Handling Editor: Petra Petra Krystek

Keywords:
Patagonian catchment
Hg partitioning
Hg speciation
Particles
Dissolved organic matter

ABSTRACT

Lake Nahuel Huapi (NH) is a large, ultraoligotrophic deep system located in Nahuel Huapi National Park (NHNP) and collecting a major headwater network of Northwestern Patagonia (Argentina). Brazo Rincón (BR), the westernmost branch of NH, is close to the active volcanic formation Puyehue-Cordón Caulle. In BR, aquatic biota and sediments display high levels of total Hg (THg), ranging in contamination levels although it is an unpolluted region. In this survey, Hg species and fractionation were assessed in association with dissolved organic matter (DOM) in several aquatic systems draining to BR. THg varied between 16.8 and 363 ng L^{-1}, with inorganic Hg (Hg^{2+}) contributing up to 99.8% and methyl mercury (MeHg) up to 2.10%. DOC levels were low (0.31–1.02 mg L^{-1}) resulting in high THg:DOC and reflecting in high Hg^{2+} availability for binding particles (partitioning coefficient log K_d up to 6.03). In streams, Hg fractionation and speciation related directly with DOM terrestrial prints, indicating coupled Hg-DOM inputs from the catchment. In the lake, DOM quality and photochemical and biological processing drive Hg fractionation, speciation and vertical levels. Dissolved gaseous Hg (Hg^0) reached higher values in BR (up to 3.8%), particularly in upper lake layers where solar radiation enhances the photoreduction of Hg^{2+} and Hg-DOM complexes. The environmental conditions in BR catchment promote Hg^{2+} binding to

* Corresponding author.
E-mail address: sotocardenasc@comahue-conicet.gob.ar (C. Soto Cárdenas).

https://doi.org/10.1016/j.chemosphere.2018.01.048

abiotic particles and bioaccumulation and the production of Hg^0, features enhancing Hg mobilization among ecosystem compartments. Overall, the aquatic network studied can be considered a "natural Hg hotspot" within NHNP.

1. Introduction

Mercury (Hg) is a global pollutant with a biogeochemical cycle involving pathways in different compartments of the Earth (Ravichandran, 2004; Selin, 2009). The atmospheric deposition of Hg (mostly Hg^{2+}) in catchments is the dominant Hg source to aquatic environments, driving the production of methyl mercury (MeHg) that biomagnifies in aquatic food webs, affecting wild life and humans through fish consumption (Chen et al., 2005; Driscoll et al., 2007, 2013; Eagles-Smith et al., 2016). The combination of local and/or regional factors (i.e. climate, landscape, vegetation cover, wetland area, etc.) can define Hg-sensitive areas and also promote wide spatial variation in Hg levels and methylation potential in aquatic systems and their biota (Driscoll et al., 2007; Brigham et al., 2009). The mobilization of Hg within watersheds is coupled with the transport of particles and dissolved organic matter (DOM), major binding agents of Hg (Grigal, 2002; Shanley et al., 2008; Dittman et al., 2010; Eagles-Smith et al., 2016). The kinetic and strength of the Hg-DOM binding depend on several environmental factors such as the concentration of particles, colloids, dissolved organic carbon (DOC), total Hg (THg), pH, among others (Haitzer et al., 2003; Adams et al., 2009; Gerbig et al., 2012). Particularly in clear, low-DOC aquatic systems, Hg speciation can be determined by photochemical reactions. These processes influence Hg fractionation, bioavailability and toxicity, by controlling the interconversion Hg^{2+}-Hg^0-Hg^{2+} and MeHg-Hg^0-MeHg, and also through changes in DOM quality and functionality related to its Hg-binding capability (Haitzer et al., 2002; Krabbenhoft et al., 2002; Fleck et al., 2014).

In Patagonia (Southern South America) headwaters are remote and pristine systems, located at both sides of the Andes, comprised in the Southern Volcanic Zone (Naranjo and Stern, 2004; Bertrand et al., 2014). Along the eastern stretch of the Patagonian Andes (Argentina) the catchments receive Hg inputs from volcanic activity, forest fires, biomass burning (Ribeiro Guevara et al., 2010; Bubach et al., 2012; Daga et al., 2008, 2014, 2016) and long-range atmospheric transport and deposition (Hermanns et al., 2013; Hermanns and Biester, 2013a,b). In lakes of Nahuel Huapi National Park (NHNP, Northwestern Patagonia, Argentina), highly variable Hg deposits have been found in sediment profiles (Arribére et al., 2008; Ribeiro Guevara et al., 2010). In the large and deep Lake Nahuel Huapi (NH) which concentrates most headwaters systems of NHNP, aquatic biota shows moderate to high total Hg (THg) levels. Large spatial differences in the THg content of lake sediments, plankton, benthos and fish have been reported among lake branches (Rizzo et al., 2014; Arcagni et al., 2017). This marked spatial pattern in Hg levels has been connected to heterogeneous Hg inputs in lake branches due to proximity to the active volcanic complex Puyehue-Cordón Caulle (PCC; last eruption 2011) as well as to branch-specific hydrogeomorphic features (i.e. lake:catchment area, soils and vegetation) (Rizzo et al., 2014; Arcagni et al., 2018). NH lake covers a sharp environmental gradient characterized by an abrupt west-east decrease in precipitation (ca. 3500–700 mm y^{-1}) and vegetation (rainforest to steppe) (Paruelo et al., 1998; Bianchi et al., 2016). The proximate lake branch to PCC, Brazo Rincón (BR), is located in a geologically-active area displaying deposits of pyroclastic materials dispersed in recent eruptions (Daga et al., 2014), gaseous seeps fields in the lake bottom (Vigliano et al., 2011) and receiving permanent atmospheric inputs of volatile pollutants including Hg (Bubach et al., 2012; Higueras et al., 2013). In BR, concentrations of THg (largely Hg^{2+}) in plankton and MeHg in benthic macroinvertebrates and fish are the highest recorded whithin NH (Rizzo et al., 2014; Arcagni et al., 2018) and thus, this branch may be considered a "natural Hg hotspot". Two main Hg pathways have been recognized in BR: i-a pelagic pathway in which dissolved Hg^{2+} is accumulated by pelagic bacteria, auto and mixotrophic protists (nanoflagellates and ciliates) and transferred to zooplankton and planktivorous fish and, ii-a benthic pathway through which MeHg is concentrated from the sediments by macroinvertebrates and transferred to foraging fish (Arcagni et al., 2018).

In this investigation, we studied Hg species along a stream-lake network draining the catchment of the BR branch of Lake NH. We studied Hg fractionation between the particulate and dissolved phases in relation to DOM in order to track sources and processes affecting Hg fate. We propose that DOM and suspended particles will be determinant of Hg fate in the stream-lake network and that photochemical and biological processes will promote Hg speciation and vertical heterogeneity in the water column of BR.

2. Materials and methods

2.1. Study site

Lake Nahuel Huapi (40°15′–41°34′ S; 71°04′–72°54′ W; Fig. 1) is a large (557 km^2) and deep (464 m maximum depth) piedmont system (764 m a.s.l.), with seven branching arms (Quirós, 1988), located inside NHNP (Patagonia, Argentina). The northwestern branch of Lake NH, called Brazo Rincón (BR), is located close to the PCC (~35 km), one of the most active volcanic complexes of the southern Andes. Lake NH is ultraoligotrophic, with low dissolved organic carbon (DOC) concentration and exposed to high levels of solar radiation (see Supplementary Material). BR branch (~12 km^2) is situated in a mountain valley surrounded by steep slopes and its catchment is ~235 km^2 (73% covered by the dense Andean-Patagonian rainforest) (Rizzo et al., 2014), resulting in a large watershed-to-lake area ratio (~20). Three mountain streams, Totoral, Pireco and South West (SW), drain the catchment towards the lake branch (Fig. 1; see Supplementary Material).

2.2. Sample collection and processing

Water samples of lotic and lentic environments were collected in November 2013 in BR catchment (Fig. 1). Three major tributary streams, Totoral, Pireco and SW, and some of their own tributaries, were surveyed at different distances from their outflow in BR. Water samples from Lake Pire were obtained in two near shore sites. BR (Z_{max} = 100 m) was sampled in a pelagic station, at nine different depths. Overall, 22 samples were obtained in this stream-lake system (Fig. 1; see Supplementary Methods for details). At each site, water samples for the determination of Hg species and DOM characterization were collected with a Kemmerer bottle suitable for

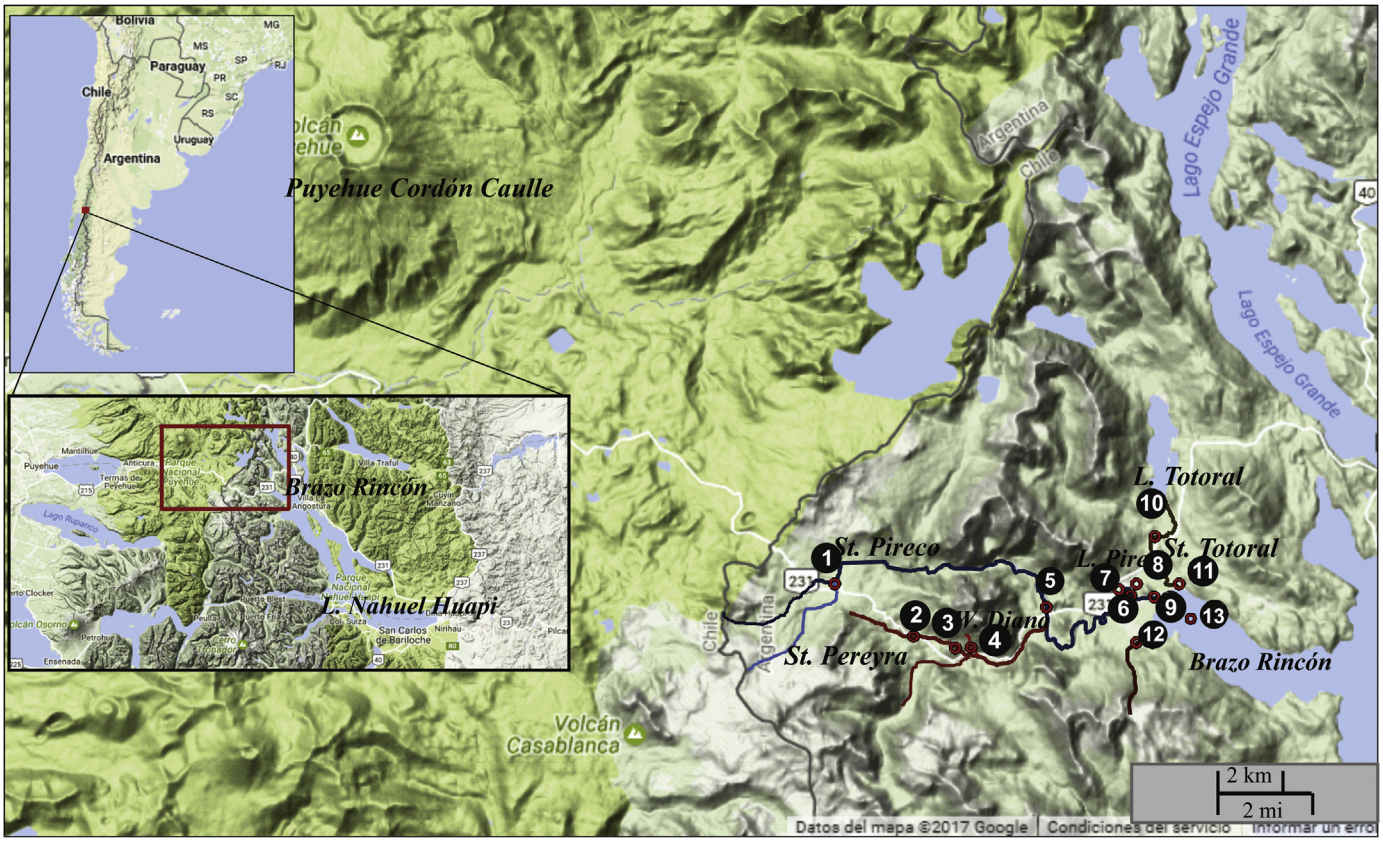

Fig. 1. Subcatchment of Brazo Rincon (BR), Lake Nahuel Huapi, Nahuel Huapi National Park (Northwestern Patagonia, Argentina). Numbers indicate the aquatic systems draining towards BR: 1) Pantojo; 2) Pereyra-2; 3) Pereyra-1; 4) Cascada Diana; 5) Pireco-1; 6) Pireco-2; 7) L Pire-1; 8) L Pire-2; 9) Pireco-3; 10) Totoral-1; 11) Totoral-2; 12) South West stream and, 13) BR sampling site. Geographic location of the sampling points and ancillary geographic data were obtained from GeoNode (National Parks Bureau, Argentina; http://mapas.parquesnacionales.gob.ar) and Google Earth® maps.

trace metal analysis. Samples for Hg and DOM analyses were poured into Teflon® (PTFE) bottles and acid-cleaned polycarbonate carboys, respectively, and transported to the laboratory thermally insulated and in darkness. At each site, temperature, dissolved oxygen (DO), pH and conductivity were measured using a multi-parameter probe (YSI 6600 V2-2).

In the laboratory, standard volumes of whole water samples were filtered through predried (20 °C) and preweighted PVDF (polyvinylidene difluoride; Millipore) membranes (0.45 μm pore size) in order to obtain the total suspended solids (TSS, particulate phase >0.45 μm) and the filtrates (dissolved and colloidal phases <0.45 μm). TSS filters were dried at room temperature in a container with silica gel. TSS' net weight was determined by subtracting the weight of the filters before and after filtration. Samples for DOM characterization were filtered through PVDF membranes (0.22 μm) and analyzed within the following 48 h after collection.

2.3. Analytical procedures

THg, MeHg, and dissolved gaseous mercury (Hg^0) concentrations were measured on unfiltered water samples. THg was also determined in TSS samples. In water samples, THg was measured after oxidation with BrCl followed by reduction with $SnCl_2$ in a cold vapor atomic absorption spectrometer (CVAAS). MeHg was determined following ethylation and back extraction, applying cold vapor atomic fluorescence (CVAF). Hg^0 was determined few hours after sampling by purging water samples, trapping Hg^0 by gold amalgamation followed by thermal desorption and CVAAS detection. THg in the particulate phase (PTHg) was determined on the TSS retained on filters after digestion with HNO_3/HF/HCl, reduced with $SnCl_2$, and detected by CVAAS. These methods are detailed in Kotnik et al. (2015, 2017). In order to control for potential contamination during samples preparation, filter blanks (PVDF) were set up by filtering a standard volume of ASTM1 water (MilliQ).

The concentrations of the filtered total mercury (FTHg), inorganic Hg (Hg^{2+}) and partition coefficient between the particulate (PTHg) and aqueous phases (FTHg) (K_d= (PTHg/FTHg) were calculated following Watras et al. (1998) and Dittman et al. (2010) (See Supplementary Methods).

Chlorophyll *a* (Chl*a*) concentration at the different depths sampled in BR was assessed by filtering 2–2.5 L whole water samples according to Nusch (1980; See Supplementary Methods).

Dissolved organic carbon (DOC) concentration was measured in filtered samples using a Shimadzu TOC-L high temperature analyzer with a high sensitivity catalyst (manufacturer's detection limit of 0.004 mg L^{-1}) (Supplementary Methods).

The chromophoric and fluorescent fractions of DOM (CDOM and FDOM, respectively) were characterized on filtered water samples using Milli-Q water as reference blank for both techniques. Absorption coefficients were calculated from absorbance scans and applied as proxies of CDOM composition (Supplementary Methods). The spectral slope for the interval of 275–295 nm ($S_{275-295}$) was applied as a surrogate of DOM molecular size relating also with photodegradation processes (Helms et al., 2008, 2013). The a_{254}:DOC ($SUVA_{254}$) and a_{350}:DOC were applied as indicators of DOM aromaticity (Weishaar et al., 2003) and lignin content (Spencer et al., 2008, 2009), respectively. The humification index (HIX; Ohno, 2002) and the biological or freshness index (BIX;

Huguet et al., 2009) were calculated to describe the relative degree of humification and autotrophic FDOM production, respectively. BIX values > 1 associate with a dominant autochthonous DOM source, those below 0.6 indicate a lower autochthonous production (Huguet et al., 2009). HIX takes values from 0 to 1, and higher values are indicative of increased DOM humification (Ohno, 2002).

Excitation-emission matrices (EEMs) were measured in filtered water samples and analyzed applying Parallel Factor Analysis (PARAFAC) to obtain DOM components (Stedmon et al., 2003; Murphy et al., 2014). Further details are provided in the Supplementary Methods.

2.4. Statistical analysis

Correlation analysis was applied to study the relationship between Hg species and DOC concentration, and DOM quality [aromaticity ($SUVA_{254}$), lignin content (a_{350}:DOC), molecular size ($S_{275-295}$), and fluorescence indexes BIX and HIX].

Multivariate analyses were carried out to explore the relationship between environmental variables and Hg species in the aquatic systems draining towards BR. First, a principal component analysis (PCA) was conducted to determine the most influential physic-chemical parameters explaining the variability among the different aquatic systems, taking into account conductivity, TSS, DOM quality proxies (a_{350}:DOC, $S_{275-295}$, $SUVA_{254}$, BIX, HIX and percentages of the fluorescent components C1, C2 and C3), and DOC concentration. All response variables were log-transformed, centered and standardized before performing the PCA. Second, a redundancy analysis (RDA) was performed to explore the relationship between physic-chemical features and Hg speciation. We analyzed the effect of TSS, DOC and DOM quality parameters on the relative contribution of Hg species in the aquatic systems. Two data matrices were used, one including TSS, DOC and DOM quality proxies (a_{350}:DOC, $S_{275-295}$, BIX, HIX and percentage of fluorescent components C1, C2 and C3) and the other including Hg response variables (log K_d, Hg^{2+}, MeHg and Hg^0). Environmental variables were log-transformed, centered and standardized. The environmental variables highly correlated with other variables were removed from the RDA when variance inflation factors (VIF) were higher than 20. The PCA and RDA analyses were performed using the software CANOCO 4.5 (ter Braak and Šmilauer, 1998), applying forward selection. Variables not contributing significantly to the model after forward selection (Hall et al., 1999) were considered as supplementary. In the RDA, the significance of the canonical axes was tested through Monte Carlo permutations (Leps and Šmilauer, 2003).

3. Results

3.1. Physic-chemical variables

In general all physic-chemical parameters differed between the streams and BR lake branch, however, streams showed a broader variation (See Supplementary Results; Table S1; Fig. S1). TSS fluctuated between 0.03 and 22.07 mg L^{-1} in the streams whereas in the lake the range was lower (0.54–1.16 mg L^{-1}) with the upper strata showing higher values (maximum at 50 m) (Fig S1c; Table S1). In the water column of BR, Chl*a* fluctuated between 0.3 and 1.2 μg L^{-1} displaying higher values up to 40 m depth (photic zone), the maximum concentration at the limit of the photic layer and decreasing downwards (Fig. S1d). DOC was overall low (0.21–1.02 mg L^{-1}) with a decreasing pattern from the streams towards the lake (Table S1). In the lake, DOC was similar in the upper and deeper strata, showing a maximum at 50 m (Fig. S1e; Table S1). CDOM and FDOM characterization indicated DOM quality differences between the streams and the lake (Supplementary Results; Table S1; Fig S2). Stream DOM showed higher aromaticity ($SUVA_{254}$), molecular weight ($S_{275-295}$), lignin content (a_{350}:DOC) and humification (HIX) and lower biological production (BIX) than lake DOM (Table S1). Three fluorescent components were identified, C1 and C2 (humic-like and terrestrially-derived compounds) and C3 (protein-like and/or aliphatic compounds) which showed different contributions in the streams and in the lake profile (Table S1; Fig. S2). Nevertheless, the C1 and C2 prevailed in all the sites (Fig. S2a–c), suggesting a high contribution of terrestrial DOM. In the lake, C1 and C2 increased downward in the profile, whereas C3 showed a higher contribution (up to 39.4%) in the upper illuminated strata (Supplementary Results; Fig. S2d; Table S1). CDOM and FDOM parameters indicated consistently a DOM quality horizontal gradient from the streams towards the lake. Also, a vertical gradient in the lake was apparent and supported by the DOM proxies $S_{275-295}$ and BIX, reflecting photodegradation and biological processes in the upper strata. This pattern was captured clearly by the PCA, which clustered separately the streams and the lake and differentiated the upper and deeper strata, based on DOC concentration, CDOM and FDOM features (Supplementary Results; Fig. S3).

3.2. Mercury in the stream-lake network

Overall, our survey showed remarkable high Hg concentrations in BR catchment. In the streams, THg varied between 40.7 and 363 ng L^{-1} (Fig. 2a left panel; Table S1). In the lake, THg levels were significantly higher in the upper layers, varying between 114 and 268 ng L^{-1} from surface to 60 m; and between 16.8 and 35.6 ng L^{-1} from 70 to 90 m ($F = 24.27$, $p < .05$; Fig. 2a, right panel). In the streams, THg varied independently of DOC ($p > .05$), however, correlated positively with DOM terrestrial signatures (lignin content and aromaticity) and negatively with DOM molecular weight (Table 1). In the lake, THg was also independent of DOC ($p > .05$), but correlated positively with the non-humic component C3 (Table 1). In general the THg:DOC ratios were high; streams showed a wider variation in THg:DOC (60.3 and 1204.4 ng mg^{-1}) compared to the lake (51.9–785 ng mg^{-1}) (Fig. S4a left panel; Table S1). In the lake profile, the upper layers displayed higher THg:DOC (Fig. S4a right panel) with a maximum value at 60 m and decreasing from 70 to 90 m (Fig. S4c; Table S1).

PTHg varied from 7.1 to 67.9 ng L^{-1} in streams and from 0.3 to 76.6 ng L^{-1} in the lake, attaining higher values in the upper strata ($F = 79.94$; $p < .05$; Fig. 2b, Table S1). In the streams, PTHg showed a positive relationship with DOM lignin content and aromaticity (Table 1). In the lake PTHg was negatively related with DOM aromaticity, lignin content, humification, C1 and C2; whereas correlated positively with DOM molecular weight, biological production, C3, TSS and Chl*a* (Table 1). Overall, these relationships indicate that lower molecular weight DOM and biological activity enhance Hg concentration in the particulate fraction.

FTHg varied between 14.6 and 303.8 ng L^{-1} in streams and between 16.51 and 202.1 ng L^{-1} in the lake, with the upper strata showing higher values than the deeper layers ($F = 10.57$; $p < .05$) (Fig. 2c; Table S1). FTHg related directly with DOM aromaticity and lignin content and negatively with the molecular weight in the streams, while in the lake was independent of DOM quality (Table 1).

The partitioning coefficient (log K_d) ranged similarly in streams and in the lake (Fig. 2d left panel), displaying higher values in the lake upper layers than in deeper ones ($F = 79.04$; $p < .001$; Fig. 2d right panel; Table S1). In the streams the log K_d correlated negatively with TSS and C2 (Table 1). In contrast, in the lake the log K_d correlated positively with TSS and also with the $S_{275-295}$, Chl*a* and

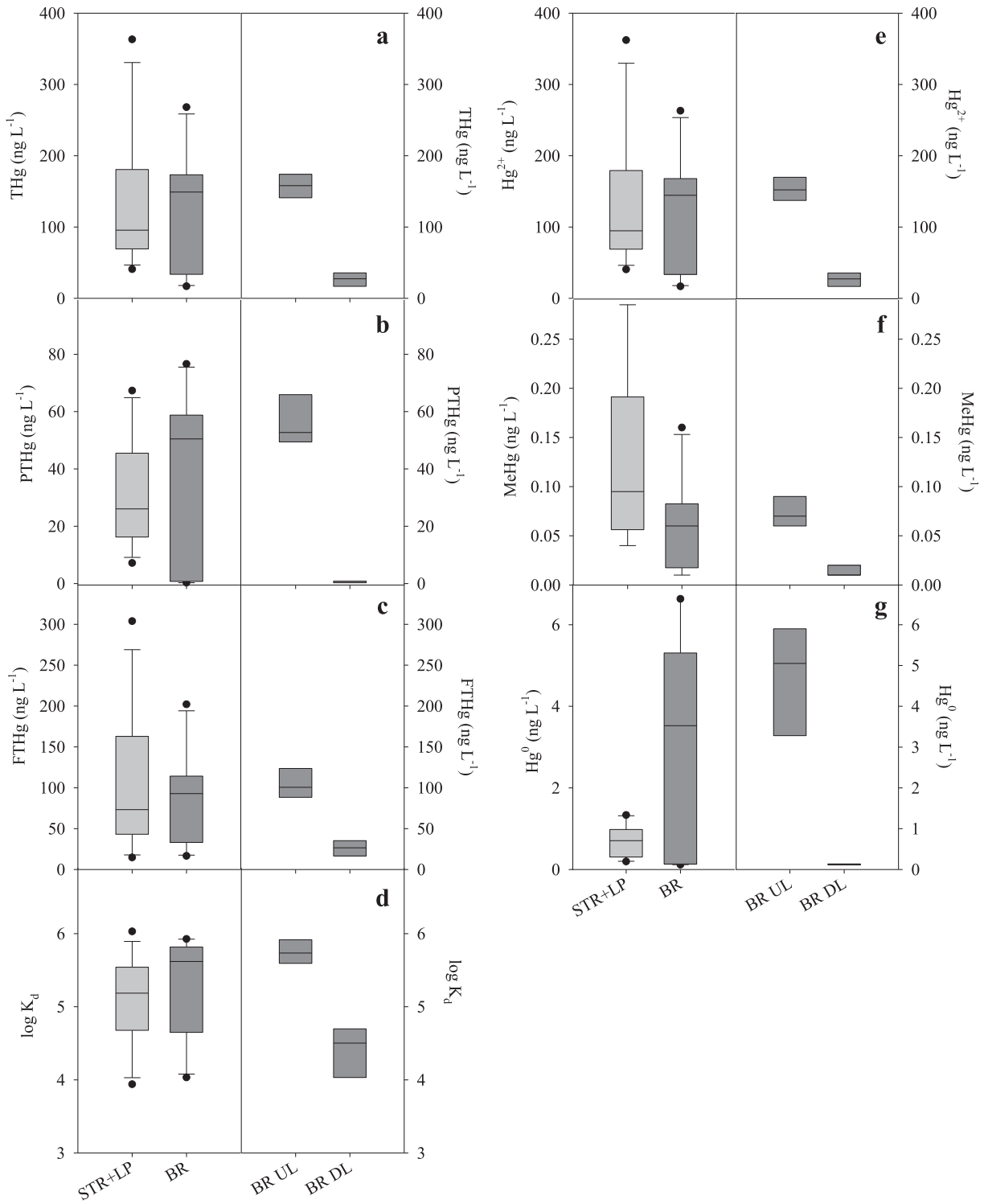

Fig. 2. Hg species concentration in the aquatic ecosystems draining BR subcatchment of Lake Nahuel Huapi: a) Total Hg (THg); b) Particulate Total Hg (PTHg); c) Filtered Total Hg (FTHg); d) Partition coefficient (log K_d) between Particulate Total Hg (PTHg) and Filtered Total Hg (FTHg); e) inorganic mercury (Hg^{2+}); f) Methyl mercury (MeHg); g) Dissolved gaseous Hg (Hg^0). References: STR + LP: Streams and L PIRE; BR: Brazo Rincón (Lake Nahuel Huapi); BR UL: Upper layers of BR (surface to 60 m depth); BR DL: Deeper layers of BR (70–90 m depth).

C3 (Table 1) reflecting a high binding of Hg to particles and an enhancement due to the biotic fraction. At the same time, the negative correlations between log K_d and terrestrial signatures (Table 1) suggest that Hg binds preferentially to DOM of higher lignin and humic content, and thus is retained in the dissolved phase.

The concentration of Hg^{2+} ranged between 16.5 and 362.1 ng L^{-1}, being higher in streams (40.4–362.1 ng L^{-1}) than in the lake (16.7–262.8 ng L^{-1}) (Fig. 2e left panel; Table S1). Prevalence of Hg^{2+} was recorded in all the systems, reaching up to 99.8%

Table 1
Pearson's correlation (r) between Total Hg (THg), Particulate Total Hg (PTHg), Filtered Total Hg (FTHg), inorganic Hg (Hg^{2+}), Methyl Hg (MeHg), Dissolved Gaseous Hg (Hg^0), and coefficient of partitioning (log K_d) and Chl*a*, Total Suspended Solids (TSS), DOC concentration, CDOM parameters ($S_{275-295}$, $SUVA_{254}$, a_{350}:DOC) and FDOM parameters (HIX, BIX) and fluorescent components in streams and BR lake branch. Significant correlations are indicated in bold ($p < .01$) and italic ($p < .05$).

		Chl*a*	TSS	DOC	$S_{275-295}$	SUVA	BIX	HIX	a_{350}:DOC	C1	C2	C3
Stream	**THg**		–	–	**−0.72**	**0.74**	–	–	**0.85**	–	–	–
	PTHg		–	–	–	**0.66**	–	–	*0.59*	–	–	–
	FTHg		–	–	**−0.75**	**0.68**	–	–	**0.82**	–	–	–
	Hg^{2+}		–	–	**−0.72**	**0.74**	–	–	**0.85**	–	–	–
	MeHg		–	–	–	**0.70**	–	–	*0.63*	–	–	–
	Hg^0		–	–	–	–	–	–	–	–	–	–
	log K_d		**−0.68**	–	–	–	–	–	–	–	*−0.56*	*0.56*
Lake	**THg**	–	–	–	–	–	–	–	–	–	–	*0.652*
	PTHg	*0.68*	*0.68*	–	*0.70*	*−0.65*	*0.62*	**−0.82**	*−0.71*	**−0.82**	*−0.71*	**0.85**
	FTHg	–	–	–	–	–	–	–	–	–	–	–
	Hg^{2+}	–	–	–	–	–	–	–	–	–	–	*0.641*
	MeHg	–	*0.70*	**0.78**	–	*−0.68*	–	–	–	–	–	–
	Hg^0	*0.64*	–	–	*0.75*	–	*0.71*	**−0.88**	*−0.67*	**−0.82**	*−0.76*	**0.89**
	log K_d	**0.81**	*0.65*	–	**0.82**	*−0.71*	–	**−0.83**	**−0.79**	**−0.93**	**−0.83**	**0.88**

of the THg (%Hg^{2+}) (Table S1). In the streams, Hg^{2+} correlated positively with DOM aromaticity, lignin content and negatively with the $S_{275-295}$ (inversely related with the molecular weight) (Table 1). In the lake, the %Hg^{2+} was slightly lower in the upper layers (96–98%) than in the deeper layers (99%) with a maximum at 60 m ($F = 23.12$; $p < .05$; Fig. 2e right panel; Table S1). Hg^{2+} showed a positive correlation with C3 predominant in the upper strata (Table 1).

The MeHg:THg (%MeHg) was overall low; however, concentrations were higher in the streams (up to 0.21%) than in the lake (up to 0.12%) (Fig. S5a,b; Table S1). In the streams, MeHg ranged from 0.01 to 0.30 ng L^{-1} whereas in the lake varied between 0.01 and 0.16 ng L^{-1} ($F = 4.45$; $p < .05$; Fig. 2f, left panel; Table S1), displaying higher values in the upper strata ($F = 9.33$; $p < .05$; Fig. 2f, right panel; Table S1). Streams showed a wider variation of the MeHg:DOC ratio (0.06–0.83 ng mg^{-1}) than the lake (0.03–0.31 ng mg^{-1}) (Fig. S4b left panel; Table S1), and the upper layers displayed higher values than deeper strata (Fig. S4d; Table 1). In the streams, MeHg was independent of DOC ($p > .05$); however, showed a positive correlation with terrigenous DOM proxies (aromaticity and lignin content). In the lake MeHg concentrations correlated positively with DOC and TSS, and negatively with DOM aromaticity (Table 1).

Hg^0 was up to four-fold higher in the lake (0.12–6.63 ng L^{-1}) than in the streams (0.19–1.33 ng L^{-1}) ($F = 17.09$; $p < .001$; Fig. 2g left panel), representing around 3.8% and 1.3% of THg (Hg^0:THg), respectively (Table S1). In the lake, Hg^0 was up to two-fold higher in the upper strata than in the depper ones (up to 3.8% and 1.9%, respectively) ($F = 32.6$; $p < .001$; Table S1; Fig. 2g right panel), correlating directly with the molecular weight, BIX, C3 and Chl*a* concentration. Low molecular weight DOM with biological contribution prevailing in the lake upper layers coincided with higher levels of Hg^0, whereas, more humic DOM signatures in deeper layers were related with lower Hg^0 levels (Table 1). In contrast, in the streams the concentration of Hg^0 was independent of CDOM and FDOM variables ($p > .05$) (Table 1).

The RDA analysis conducted with Hg species relative to THg as response variables and DOM concentration and quality parameters as environmental variables, explained 99.2% of the dataset variation (axis 1 = 94.1%; axis 2 = 5.1%) (Fig. 3). DOM quality parameters separated the upper from the deeper layers of the lake and the streams. Axis 1 showed a gradient of DOM quality associating higher levels of Hg^{2+} and MeHg in the streams and deeper layers of the lake to predominantly terrigenous DOM proxies (lignin content, humification and humic components C1 and C2) (Fig. 3). Besides, the upper layers of the lake clustered apart, with higher Hg^0 values and high partitioning (log K_d) associated with non-humic, low molecular weight DOM (component C3 and $S_{275-295}$). Axis 2 correlated negatively with DOC and positively with the lignin content (Fig. 3).

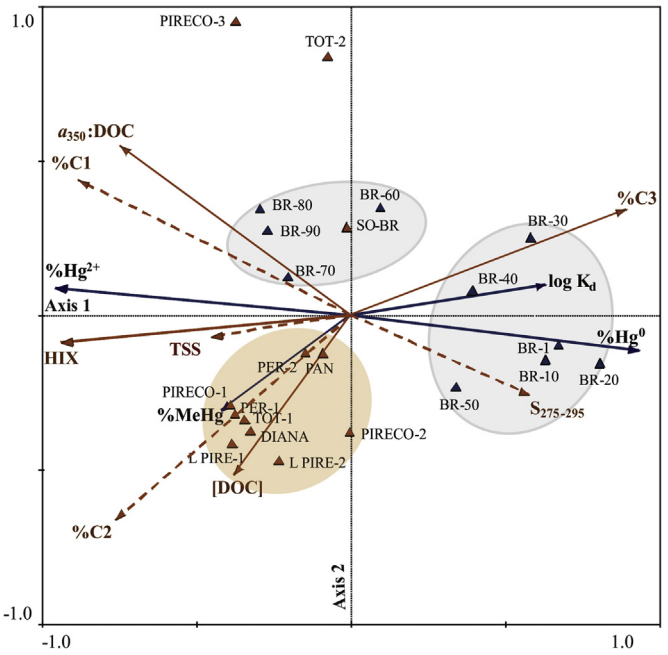

Fig. 3. Redundancy analysis (RDA) including DOC, total suspended solids (TSS), DOM quality proxies (a_{350}:DOC, $S_{275-295}$, HIX, percentage of fluorescent components C1, C2 and C3) as environmental variables and percentage of Hg species (Hg^{2+}, MeHg) and Hg^0) and the partition coefficient (log K_d) as response variables (blue arrows). Significant (light brown solid arrows) and non-significant (light brown dashed arrows) environmental variables are indicated. References: PAN: Pantojo; PER-1, PER-2: Pereyra stream, DIANA: Cascada Diana; PIRECO-1, PIRECO-2, PIRECO-3: Pireco stream; L PIRE-1, L PIRE-2: Pire lake; TOT-1; TOT-2: Totoral stream; SW: South West stream; BR: sampling depth. (For interpretation of the references to colour in this figure legend, the reader is referred to the Web version of this article.)

4. Discussion

The aquatic systems of the BR catchment characterize by their low DOC concentrations (Table S1) with a high contribution of terrestrial DOM. At the time of this survey, the BR catchment was the area of NHNP showing the highest impact of a recent eruption (2011) of the PCC complex, characterized by high deposition and loads of volcanic ash. This reflected in most aquatic systems close to

the PCC, which showed increased TSS, turbidity and phosphorus concentration (Modenutti et al., 2013; Balseiro et al., 2014; Lallement et al., 2014). In fact, TSS was particularly high in the studied streams, whereas in the lake higher values were recorded up to 60 m showing the contribution of planktonic algae, as reflected by the positive relationship between TSS and Chl*a*.

In BR catchment, moderate to high THg concentrations were measured (16.8–363 ng L^{-1}) and Hg^{2+} was found as the prevailing species accounting up to 99.8% of THg. In contrast, MeHg concentrations were extremely low, representing less than 2% of THg (Table S1). The THg and high Hg^{2+} levels recorded in this study can be considered within those present in contaminated unproductive surface waters in forested regions of North America with high Hg deposition (Driscoll et al., 2007; Eagles-Smith et al., 2016). However, the low MeHg levels found in the BR catchment may be due to the combination of small wetlands' surface, high precipitation, low temperature and steep slopes that promotes the rapid runoff, preventing Hg methylation in soil and streambeds. The production of MeHg can vary widely under conditions of high THg loading, depending on the methylation efficiency of a particular ecosystem (Krabbenhoft et al., 1999; Driscoll et al., 2007).

The direct association of different Hg fractions (PTHg and FTHg) and species (THg, Hg^{2+} and MeHg) with terrestrial DOM signatures highlighted the major contribution of the catchment. Downslope in the lake branch, Hg speciation and fractionation in the depth profile seemed to be controlled by a combination of factors such as DOM quality, exposure to sunlight, biological uptake, microbial processes and interactions with lake sediments, favored by the higher water residence time. Particularly, MeHg was very low in the water column of BR, although slightly higher levels were recorded in the upper layers. This pattern may indicate a positive balance between abiotic methylation and demethylation processes, which in mountain lakes are favored by high underwater UV levels (Krabbenhoft et al., 2002; Graham et al., 2013; Fleck et al., 2014). MeHg showed a positive correlation with TSS but was unrelated with Chl*a*, suggesting that bacteria and the abiotic fraction of TSS also scavenge this Hg species. Thus, particles and DOM play a major role in the entrance, fractionation and speciation of Hg in the studied catchment. In fact, DOM quality allowed tracking accurately the source and the processes affecting Hg in the studied systems. The high flow and steep slopes of these low order streams produce the rapid downstream transport of particulate and dissolved materials preventing in-stream processing (i.e. photobleaching), as has been observed in nearby systems (Albariño et al., 2009; Garcia et al., 2015). Consequently, stream DOM displays terrestrial prints and low processing, while in contrast, lake DOM shows clear signals of photochemical and biological processing (i.e. higher C3 and BIX, lower $S_{275–295}$, among others), especially in the upper layers (Fig. S3).

In general the systems surveyed have extremely low DOC concentrations, and high THg levels, resulting in high to very high THg:DOC ratios (Table S1; Fig. S4a). In a range of natural waters, THg:DOM ratios have been reported to take values between 0.01 and 10 ng mg^{-1} (Haitzer et al., 2002; Mitchell et al., 2008; Zheng and Hintelmann, 2009), remarkably lower values than those calculated for our systems. DOC affects the supply and bioavailability of Hg in aquatic systems (Ravichandran, 2004; Gorski et al., 2008; Luengen et al., 2012). The THg:DOC ratio determines the sorption of Hg to aquatic particles and dissolved compounds, which are known to influence the kinetics of Hg reduction, the transference of Hg to the sediments and its entry to food webs (Zheng and Hintelmann, 2009). Overall, the low DOC levels and high Hg^{2+} concentrations in the studied systems promote a high adsorption of Hg^{2+} to abiotic and biotic particles, as indicated by the high log K_d and high PTHg. In fact, the fractionation of Hg between the dissolved and particulate phases was high and related mainly with TSS, DOC and DOM quality (Table S1). In streams, the increase in TSS decreased the adsorption of Hg into particles, which has been described in the literature as “particle concentration effect” (Babiarz et al., 2001; Adams et al., 2009; Dittman et al., 2010).

The coupled dynamics of Hg, particles and DOM showed some interesting patterns in the water column of the lake. In the profile, the concentration of PTHg related negatively with terrestrial DOM proxies (Table 1; Fig. 3). In the upper layers DOM signatures reflected photochemical degradation and biological processing. Higher levels of PTHg were recorded in the upper strata, likely due to the patchy distribution of pelagic algae, as indicated by the positive correlation between Chl*a* and PTHg. In contrast, in the deeper layers, PTHg was lower which may relate to the fact that the prevailing humic DOM retains Hg in the dissolved phase and also due to the lower contribution of algae to the TSS. Particle surface quality can be a critical factor controlling Hg fractionation, with organic coats in biotic particles providing more binding sites than inorganic ones (Chadwick et al., 2013; Jang et al., 2014; Soto Cárdenas et al., 2014). In fact, pelagic organisms, including bacteria, phyto and zooplankton bioaccumulate Hg^{2+} actively and passively from the dissolved phase in natural low DOC water of different lakes of NHNP (Diéguez et al., 2013; Soto Cárdenas et al., 2014).

The photoreduction of Hg^{2+}-DOM complexes was clearly indicated by the negative relationship between Hg^0 and terrestrial DOM proxies, and was also supported by the positive relationship with $S_{275–295}$, a proxy of DOM photochemical processing. In the upper layers of the lake, DOM characterized by low molecular weight, low aromaticity, relatively lower contribution of humic compounds and clear signals of photodegradation. In Andean lakes, the high penetration of solar radiation and UV levels promote photochemical reactions in the upper layers conducting to DOM breakdown, reflected in CDOM and FDOM photobleaching (Zagarese et al., 2001; Soto Cárdenas et al., 2017). In low DOC, highly transparent waters, photochemical weathering contributes to DOM break down enhancing C mineralization and the generation of photo-reactive intermediates that can influence the redox state of Hg (García et al., 2005; Haverstock et al., 2012; He et al., 2012).

Several investigations have reported the photoproduction of Hg^0 depending on the availability of photo-reducible Hg^{2+}, which in turn is regulated by the THg:DOC ratio (Haitzer et al., 2002; Zheng and Hintelmann, 2009). In our systems the high THg:DOC ratios and the impact of photochemical reactions in the upper layers (Morris et al., 1995; Zagarese et al., 2001) may conduct to a relatively low stability of the Hg–DOM complexes leading to higher photoreduction rates and higher Hg^0 levels in the upper layers of the lake. At high THg:DOC ratios the stability of Hg^{2+}–DOM complexes decreases sharply, thereby enhancing the potential for Hg^{2+} reduction (Haitzer et al., 2002). Additionally, the positive relationship between Hg^0 and Chl*a* indicated that photosynthetic organisms concentrated in the upper strata enhanced Hg^0 production. Phototrophic organisms can reduce Hg in processes dependent on the generation of reductants inside the cells and/or on the excretion of reductants into the surrounding water (Ben-Bassat and Mayer, 1978; Poulain et al., 2004; Lanzillotta et al., 2004). Interestingly, in Lake NH the accumulation of Hg^{2+} in small planktonic fractions including autotrophic and mixotrophic species is extremely high (Rizzo et al., 2014; Arcagni et al., 2017). Thus, the production of Hg^0 by photosynthetic organisms could add to Hg reduction in the water column. Further, the extremely windy conditions of the Patagonian region affect the rates and distribution of photoreactions in the water column (Zagarese et al., 2001), which could favor Hg^0 production, eventually enhancing Hg^0 emission to the atmosphere, as has been shown by Garcia et al. (2005). The Hg^0

production and the subsequent emission to the atmosphere represents a significant pathway for reducing the level of this potentially toxic element in aquatic ecosystems.

5. Conclusions

The aquatic network draining BR catchment can be considered a "natural Hg hotspot" within NHNP because THg in water and biota are the highest within the lake, reaching levels found in contaminated sites. BR catchment is densely forested, has the highest precipitation of the area, and is characterized by a high watershed:lake area. The steep slopes determine the fast downstream transport of terrestrial DOM and Hg species towards the lake. THg in the studied systems is moderate to high (16.8–363 ng L^{-1}; 96–99.8% Hg^{2+}) whereas MeHg is overall low (up to 2.10%) having a terrestrial origin. DOC concentrations in the studied systems are extremely low (0.31–1.02 mg L^{-1}) resulting in very high THg:DOC. This condition determines a high tendency of Hg to bind abiotic and biotic particles (log K_d 3.94–6.03), promoting its transference into food webs and the mobilization within the ecosystem, i.e. water column-bottom (sedimentation); water column-atmosphere (photo and bioreduction and emission). In the water column, Hg, DOM and particles are subjected to biological and photochemical reactions acting differentially in the upper and deeper layers. High Hg^{2+} levels and photochemical processes affecting DOM-Hg complexes could promote the dynamic generation of Hg^0 and abiotic methylation and demethylation, especially in the upper layers. Additionally, pelagic photosynthetic organisms intervene in the cycling of Hg since they scavenge dissolved Hg^{2+} and incorporate it in the pelagic food web, mobilize Hg to the sediments through senescence and sinking, and mineralize Hg^{2+} contributing to Hg^0 production and export.

Acknowledgements

National Parks Bureau of Argentina granted permission to sample Lake Nahuel Huapi. We are grateful to Dr. P.E. García for conducting the PARAFAC analysis. This investigation was funded by PICT 2015-3496/2016-0499 and UNComahue 04/B194. C. Soto Cárdenas is a CONICET postdoctoral fellow, M.C. Diéguez, A. Rizzo and C. Queimaliños are CONICET researchers and Sergio Ribeiro Guevara is a CNEA researcher.

Appendix A. Supplementary data

Supplementary data related to this article can be found at https://doi.org/10.1016/j.chemosphere.2018.01.048.

References

Adams, R.M., Twiss, M.R., Driscoll, C.T., 2009. Patterns of mercury accumulation among seston in lakes of the adirondack mountains, New York. Evol. Sci. Technol. 43, 4836–4842.
Albariño, R.J., Díaz Villanueva, V., Buria, L., 2009. Leaf Litter Dynamics in a Forested Small Andean Catchment, Northern Patagonia, Argentina. Ecological Advances on Chilean Temperate Rainforests. Academia Press, Ghent, Belgium, pp. 183–211.
Arcagni, M., Rizzo, A., Juncos, R., Pavlin, M., Campbell, L.M., Arribére, M.A., Horvat, M., Ribeiro Guevara, S., 2017. Mercury and selenium in the food web of lake Nahuel Huapi, Patagonia, Argentina. Chemosphere 166, 163–173.
Arcagni, M., Juncos, R., Rizzo, A., Pavlin, M., Fajon, V., Arribére, M.A., Horvat, M., Ribeiro Guevara, S., 2018. Species- and habitat-specific bioaccumulation of total mercury and methylmercury in the food web of a deep oligotrophic lake. Sci. Total Environ. 612, 1311–1319.
Arribére, M.A., Ribeiro Guevara, S., Bubach, D.F., Arcagni, M., Vigliano, P.H., 2008. Selenium and mercury in native and introduced fish species of Patagonian lakes, Argentina. Biol. Trace Elem. Res. 122, 43–63.
Babiarz, C.L., Hurley, J.P., Hoffman, S.R., Andren, A.W., Shafer, M.M., Armstrong, D.E., 2001. Partitioning of total mercury and methyl- mercury to the colloidal phase in freshwaters. Evol. Sci. Technol. 35, 4773–4782.
Balseiro, E., Souza, M.S., Serra Olabuenaga, I., Wolinski, L., Bastidas Navarro, M., Laspoumaderes, C., Modenutti, B., 2014. Effect of the Puyehue-Cordón Caulle volcanic complex eruption on crustacean zooplankton of Andean lakes. Ecol. Austral 24, 75–82.
Ben-Bassat, D., Mayer, A.M., 1978. Light-induced Hg volatilization and evolution in *Chlorella* and the effect of DCMU and Methylamine. Physiol. Plant 42, 33–38.
Bertrand, S., Daga, R., Bedert, R., Fontijn, K., 2014. Deposition of the 2011–2012 Cordón Caulle tephra (Chile, 40°S) in lake sediments: implications for tephrochronology and volcanology. J. South Am. Earth Sci. 49, 1–14.
Bianchi, E., Villalba, R., Viale, M., Couvreux, F., Marticorena, R., 2016. New precipitation grids for Northern Patagonia: advances in relation to global climate grids. J. Meteor. Res. 30, 38–52.
Brigham, M.E., Wentz, D.A., Aiken, G.R., Krabbenhoft, D.P., 2009. Mercury cycling in stream ecosystems. 1. Water column chemistry and transport. Environ. Sci. Technol. 43, 2720–2725.
Bubach, D., Pérez Catán, S., Arribére, M.A., Ribeiro Guevara, S., 2012. Bioindication of volatile elements emission by the Puyehue-Cordón Caulle (North Patagonia) volcanic event in 2011. Chemosphere 88, 584–590.
Chadwick, S.P., Babiarz, C.L., Hurley, J.P., Armstrong, D.E., 2013. Importance of hypolimnetic cycling in aging of "new" mercury in a northern temperate lake. Sci. Total Environ. 448, 176–188.
Chen, C.Y., Stemberger, R.S., Kamman, N.C., Mayes, B.M., Folt, C.L., 2005. Patterns of Hg bioaccumulation and transfer in aquatic food webs across multi-lake studies in the Northeast US. Ecotoxicology 14, 135–147.
Daga, R., Ribeiro Guevara, S., Sánchez, M.L., Arribére, M., 2008. Source identification of volcanic ashes by geochemical analysis of well preserved lacustrine tephras in. Nahuel Huapi National Park. Appl. Radiat. Isot 66, 1325–1336.
Daga, R., Ribeiro Guevara, S., Poire, D.G., Arribére, M., 2014. Characterization of tephras dispersed by the recent eruptions of volcanoes calbuco (1961), chaitén (2008) and cordón Caulle complex (1960 and 2011) in northern Patagonia. J. South Am. Earth Sci. 49, 1–14.
Daga, R., Ribeiro Guevara, S., Pavlin, M., Rizzo, A., Lojen, S., Vreča, P., Horvat, M., Arribére, M., 2016. Historical records of mercury in southern latitudes over 1600 years: lake Futalaufquen. Northern Patagonia. Sci. Total Environ 553, 541–550.
Diéguez, M.C., Queimaliños, C.P., Ribeiro Guevara, S., Marvin-DiPasquale, M., Soto Cárdenas, C., Arribére, M.A., 2013. Influence of dissolved organic matter character on mercury incorporation by planktonic organisms: an experimental study using oligotrophic water from Patagonian lakes. J. Environ. Sci. 25, 1980–1991.
Dittman, J.A., Shanley, J.B., Driscoll, C.T., Aiken, G.R., Chalmers, A.T., Towse, J.E., Selvendiran, P., 2010. Mercury dynamics in relation to dissolved organic carbon concentration and quality during high flow events in three northeastern U.S. streams. Water Resour. Res. https://doi.org/10.1029/2009WR008351.
Driscoll, C.T., Han, Y.J., Chen, C.Y., Evers, D.C., Lambert, K.F., Holsen, T.M., Kamman, N.C., Munson, R.K., 2007. Mercury contamination in forest and freshwater ecosystems in the Northeastern United States. Bioscience 57, 17–28.
Driscoll, C.T., Mason, R.P., Chan, H.M., Jacob, D.J., Pirrone, N., 2013. Mercury as a global pollutant: sources, pathways, and effects. Environ. Sci. Technol. 47, 4967–4983.
Eagles-Smith, C.A., Wiener, J.G., Eckley, C.S., Willacker, J.J., Evers, D.C., Marvin-DiPasquale, M., Obrist, D., Fleck, J.A., Aiken, G.R., Lepak, J.M., Jackson, A.K., Webster, J.P., Stewart, A.R., Davis, J.A., Alpers, C.N., Ackerman, J.T., 2016. Mercury in western North America: a synthesis of environmental contamination, fluxes, bioaccumulation, and risk to fish and wildlife. Sci. Total Environ. 568, 1213–1226.
Fleck, J.A., Gill, G., Bergamaschi, B.A., Kraus, T.E.C., Downing, B.D., Alpers, C.N., 2014. Concurrent photolytic degradation of aqueous methyl mercury and dissolved organic matter. Sci. Total Environ. 484, 263–275.
Garcia, E., Poulain, A.J., Amyot, M., Ariya, P.A., 2005. Diel variations in photoinduced oxidation of Hg^0 in freshwater. Chemosphere 59, 977–981.
Garcia, R.D., Reissig, M., Queimaliños, C.P., Garcia, P.E., Diéguez, M.C., 2015. Climate-driven terrestrial inputs in ultraoligotrophic mountain streams of Andean Patagonia revealed through chromophoric and fluorescent dissolved organic matter. Sci. Total Environ. 521, 280–292.
Gerbig, C.A., Ryan, J.N., Aiken, G.R., 2012. The effects of dissolved organic matter on mercury biogeochemistry. In: Liu, G., Cai, Y., O'Driscoll, N.O. (Eds.), Environmental Chemistry and Toxicology of Mercury. Wiley, New York, pp. 259–292.
Gorski, P.R., Armstrong, D.E., Hurley, J.P., Krabbenhoft, D.P., 2008. Influence of natural dissolved organic carbon on the bioavailability of mercury to a freshwater alga. Environ. Pollut. 154, 116–123.
Graham, A.M., Aiken, G.R., Gilmour, C.C., 2013. Effect of dissolved organic matter source and character on microbial Hg methylation in Hg–S–DOM solutions. Environ. Sci. Technol. 47, 5746–5754.
Grigal, D.F., 2002. Inputs and outputs of mercury from terrestrial watersheds: a review. Environ. Rev. 10, 1–39.
Haitzer, M., Aiken, G.R., Ryan, J.N., 2002. Binding of mercury (ii) to dissolved organic matter: the role of the mercury-to-dom concentration ratio binding of mercury (ii) to dissolved organic matter: the role of the mercury to DOM concentration ratio. Environ. Sci. Technol. 36, 3564–3570.
Haitzer, M., Aiken, G.R., Ryan, J.N., 2003. Binding of mercury (ii) to aquatic humic substances: influence of pH and source of humic substances. Environ. Sci. Technol. 37, 2436–2441.
Hall, R.I., Leavitt, P.R., Quinlan, R., Dixit, A.S., Smol, J.P., 1999. Effects of agriculture, urbanization, and climate on water quality in the northern Great Plains. Limnol.

Oceanogr. 44, 739–756.
Haverstock, S., Sizmur, T., Murimboh, J., O'Driscoll, N.J., 2012. Modeling the photo-oxidation of dissolved organic matter by ultraviolet radiation in freshwater lakes: implications for mercury bioavailability. Chemosphere 88, 1220–1226.
He, F., Zheng, W., Liang, L., Gu, B., 2012. Mercury photolytic transformation affected by low-molecular-weight natural organics in water. Sci. Total Environ. 416, 429–435.
Helms, J.R., Stubbins, A., Ritchie, J.D., Minor, E.C., Kieber, D.J., Mopper, K., 2008. Absorption spectral slopes and slope ratios as indicators of molecular weight, source, and photobleaching of chromophoric dissolved organic matter. Limnol. Oceanogr. 53, 955–969.
Helms, J.R., Stubbins, A., Perdue, E.M., Green, N.W., Chen, H., Mopper, K., 2013. Photochemical bleaching of oceanic dissolved organic matter and its effect on absorption spectral slope and fluorescence. Mar. Chem. 115, 81–91.
Hermanns, Y.M., Biester, H., 2013a. A 17,300-year record of mercury accumulation in a pristine lake in southern Chile. J. Paleolimnol. 49, 547–561.
Hermanns, Y.M., Biester, H., 2013b. Anthropogenic mercury signals in lake sediments from southernmost Patagonia, Chile. Sci. Total Environ. 445–446, 126–135.
Hermanns, Y.M., Martinez Cortizas, A., Arz, H., Stein, R., Biester, H., 2013. Untangling the influence of in-lake productivity and terrestrial organic matter flux on 4,250 years of mercury accumulation in Lake Hambre, Southern Chile. J. Paleolimnol. 49, 563–573.
Higueras, P., Oyarzun, R., Kotnik, J., Esbrí, M.J., Martínez-Coronado, A., Horvat, M., López-Berdonces, M.A., Llanos, W., Vaselli, O., Nisi, B., Mashyanov, N., Ryzov, V., Spiric, Z., Panichev, N., McCrindle, R., Feng, X., Fu, X., Lillo, J., Loredo, J., García, M.E., Alfonso, P., Villegas, K., Palacios, S., Oyarzún, J., Maturana, H., Contreras, F., Adams, M., Ribeiro Guevara, S., Niecenski, L.F., Giammanco, S., Huremovic, J., 2013. A compilation of field surveys on gaseous elemental mercury (GEM) from contrasting environmental settings in Europe, South America, South Africa and China: separating fads from facts. Environ. Geochem. Health. https://doi.org/10.1007/s10653-013-9591-2.
Huguet, A., Vacher, L., Relexans, S., Saubusse, S., Froidefond, J.M., Parlanti, E., 2009. Properties of fluorescent dissolved organic matter in the Gironde Estuary. Org. Geochem. 40, 706–719.
Jang, J., Kim, H., Han, S., 2014. Influence of microorganism content in suspended particles on the particle-water partitioning of mercury in semi -enclosed coastal waters. Sci. Total Environ. 470–471, 1558–1564.
Kotnik, J., Horvat, M., Ogrinc, N., Fajon, V., Žagar, D., Cossa, D., Sprovieri, F., Pirrone, N., 2015. Mercury speciation in the adriatic sea. Mar. Pollut. Bull. https://doi.org/10.1016/j.marpolbul.2015.05.037.
Kotnik, J., Horvat, M., Begu, E., Shlyapnikov, Y., Sprovieri, F., Pirrone, N., 2017. Dissolved gaseous mercury (DGM) in the Mediterranean Sea: spatial and temporal trends. Mar. Chem. 193, 8–19.
Krabbenhoft, D.P., Wiener, J.G., Brumbaugh, W.G., Olson, M.L., DeWild, J.F., Sabin, T.J., 1999. A national pilot study of mercury contamination of aquatic ecosystems along multiple gradients. In: Morganwalp, D.W., Buxton, H.T. (Eds.), US Geological Survey Toxic Substances Hydrology Program: Proceedings of the Technical Meeting, Charleston, South Carolina, March 8–12, 1999, Vol. 2. Contamination of Hydrologic Systems and Related Ecosystems, pp. 147–160. US Geological Survey Water-Resources Investigations Report no. 99-4018B. (18 December 2006. http://toxics.usgs.gov/pubs/wri99-4018/Volume2.
Krabbenhoft, D.P., Olson, M.L., Dewild, J.F., Clow, D.W., Striegl, R.G., Dornblaser, M.M., Vanmetre, P., 2002. Mercury loading and methylmercury production and cycling in high-altitude lakes from the western United States. Water Air Soil Pollut. 2, 233–249.
Lallement, M.E., Juárez, S.M., Macchi, P.J., Vigliano, P.H., 2014. Puyehue Cordón-Caulle: post-eruption analysis of changes in stream benthic fauna of Patagonia. Ecol. Austral 24, 64–74.
Lanzillotta, E., Ceccarini, C., Ferrara, R., Dini, F., Banchetti, R., 2004. Importance of the biogenic organic matter in photo-formation of dissolved gaseous mercury in a culture of the marine diatom *Chaetoceros* sp. Sci. Total Environ. 318, 211–221.
Leps, J., Šmilauer, T., 2003. Multivariate Analysis of Ecological Data Using CANOCO. Cambridge University Press, Cambridge.
Luengen, A.C., Fisher, N.S., Bergamaschi, B.A., 2012. Dissolved organic matter reduces algal accumulation of methylmercury. Environ. Toxicol. Chem. 31, 1712–1719.
Mitchell, C.P.J., Branfireun, B.A., Kolka, R.K., 2008. Total mercury and methylmercury dynamics in upland–peatland watersheds during snowmelt. Biogeochemistry (Dordr.) 90, 225–241.
Modenutti, B.E., Balseiro, E.G., Elser, J.J., Bastidas Navarro, M., Cuassolo, F., Laspoumaderes, C., Souza, M.S., Díaz Villanueva, V., 2013. Effect of volcanic eruption on nutrients, light, and phytoplankton in oligotrophic lakes. Limnol. Oceanogr. 58, 1165–1175.
Morris, D.P., Zagarese, H.E., Williamson, C.E., Balseiro, E.G., Hargreaves, B.R., Modenutti, B.E., Moeller, R., Queimaliños, C., 1995. The attenuation of UV radiation in lakes and the role of dissolved organic carbon. Limnol. Oceanogr. 40, 1381–1391.
Murphy, K.R., Stedmon, C.A., Wenig, P., Bro, R., 2014. OpenFluor an online spectral library of auto-fluorescence by organic compounds in the environment. Anal. Methods 6, 658–661.
Naranjo, J., Stern, C., 2004. Holocene tephrochronology of the southernmost part (42°30'45"S) of the andean southern volcanic zone. Rev. Geol. Chile 31, 225–240.
Nusch, E.A., 1980. Comparison of different methods for chlorophyll and pheopigment determination. Arch. Hydrobiol. 14, 14–36.
Ohno, T., 2002. Fluorescence inner-filtering correction for determining the humification index of dissolved organic matter. Environ. Sci. Technol. 36, 742–746.
Paruelo, J.M., Beltran, A., Jobbágy, E., Sala, O.E., Golluscio, R.A., 1998. The climate of Patagonia: general patterns and controls on biotic processes. Ecol. Austral 8, 85–101.
Poulain, A.J., Amyot, M., Findlay, D., Telor, S., Barkay, T., Hintelmann, H., 2004. Biological and photochemical production of dissolved gaseous mercury in a boreal lake. Limnol. Oceanogr. 49, 2265–2275.
Quirós, R., 1988. Relationships between air temperature, depth, Nutrients and Chlorophyll in 103 Argentinian lakes. Verh. Int. Ver. Theor. Angew. Limnol 23, 647–658.
Ravichandran, M., 2004. Interactions between mercury and dissolved organic matter – a review. Chemosphere 55, 319–331.
Ribeiro Guevara, S., Meili, M., Rizzo, A., Daga, R., Arribére, M., 2010. Sediment records of highly variable mercury inputs to mountain lakes in Patagonia during the past millennium. Atmos. Chem. Phys. 10, 3443–3453.
Rizzo, A., Arcagni, M., Campbell, L.M., Koron, N., Pavlin, M., Arribére, M.A., Horvat, M., Ribeiro Guevara, S., 2014. Source and trophic transfer of mercury in plankton from an ultraoligotrophic lacustrine system (Lake Nahuel Huapi, North Patagonia). Ecotoxicology 23, 1184–1194.
Selin, N.E., 2009. Global biogeochemical cycling of mercury: a review. Annu. Rev. Environ. Resour. 34, 43–63.
Shanley, J.B., Mast, M.A., Campbell, D.H., Aiken, G.R., Krabbenhoft, D.P., Hunt, R.J., Walker, J.F., Schuster, P.F., Chalmers, A., Aulenbach, B.T., Peters, N.E., Marvin-DiPasquale, M., Clow, D.W., Shafer, M.M., 2008. Comparison of total mercury and methylmercury cycling at five sites using the small watershed approach. Environ. Pollut. 154, 143–154.
Soto Cárdenas, C., Diéguez, M.C., Ribeiro Guevara, S., Marvin-DiPasquale, M., Queimaliños, C.P., 2014. Incorporation of inorganic mercury (Hg^{2+}) in pelagic food webs of ultraoligotrophic and oligotrophic lakes: the role of different plankton size fractions and species assemblages. Sci. Total Environ. 494–495, 65–73.
Soto Cárdenas, C., Gerea, M., Garcia, P.E., Pérez, G.L., Diéguez, M.C., Rapacioli, R., Reissig, M., Queimaliños, C., 2017. Interplay between climate and hydrogeomorphic features and their effect on the seasonal variation of dissolved organic matter in shallow temperate lakes of the Southern Andes (Patagonia, Argentina): a field study based on optical properties. Ecohydrology. https://doi.org/10.1002/eco.1872.
Spencer, R.G.M., Aiken, G.R., Wickland, K.P., Striegl, R.G., Hernes, P.J., 2008. Seasonal and spatial variability in dissolved organic matter quantity and composition from the Yukon River basin, Alaska. Global Biogeochem. Cycles 22, GB4002. https://doi.org/10.1029/2008GB003231.
Spencer, R.G.M., Aiken, G.R., Butler, K.D., Dornblaser, M.M., Striegl, R.G., Hernes, P.J., 2009. Utilizing chromophoric dissolved organic matter measurements to derive export and reactivity of dissolved organic carbon exported to the Arctic Ocean: a case study of the Yukon River, Alaska. Geophys. Res. Lett. 36, L06401.
Stedmon, C.A., Markager, S., Bro, R., 2003. Tracing dissolved organic matter in aquatic environments using a new approach to fluorescence spectroscopy. Mar. Chem. 82, 239–254.
ter Braak, C.J.F., Šmilauer, P., 1998. CANOCO Reference Manual and User's Guide to Canoco for Windows – Software for Canonical Community Ordination. Microcomputer Power, Ithaca, NY, version 4. .
Vigliano, P.H., Jones, A., Judd, A., Planas, H., Lippolt, G., 2011. Bottom gas seeps at lake Nahuel Huapi, Patagonia. Rev. Asoc. Geol. Argent. 68, 481–490.
Watras, C.J., Back, R.C., Halvorsen, S., Hudson, R.J.M., Morrison, K.A., Wente, S.P., 1998. Bioaccumulation of mercury in pelagic freshwater food webs. Sci. Total Environ. 219, 183–208.
Weishaar, J.L., Aiken, G.R., Bergamaschi, B.A., Fram, M.S., Fujii, R., Mopper, K., 2003. Evaluation of specific ultraviolet absorbance as an indicator of the chemical composition and reactivity of dissolved organic carbon. Environ. Sci. Technol. 37, 4702–4708.
Zagarese, H.E., Diaz, M., Pedrozo, F., Ferraro, M., Cravero, W., Tartarotti, B., 2001. Photodegradation of natural organic matter exposed to fluctuating levels of solar radiation. J. Photochem. Photobiol. B Biol. 61, 35–45.
Zheng, W., Hintelmann, H., 2009. Mercury isotope fractionation during photoreduction in natural water is controlled by its Hg/DOC ratio. Geochim. Cosmochim 73, 6704–6715.